Nordic Energy Research Programme Norwegian U. of Science and Technology

Oil Recovery in Fractured Reservoirs

Arne Graue, Robert W. Moe and Thomas Bognø
Department of Physics, University of Bergen, Norway

Abstract
Visualization of the effects of various wettability conditions on oil recovery in fractured reservoirs is demonstrated in two-dimensional in-situ imaging experiments in large blocks of chalk and by numerical simulations. Recovery mechanisms are shown to change with a change in wettability. Iterative comparison between experimental work and numerical simulations has been used to predict oil recovery mechanisms in fractured chalk as a function of wettability. Selective alteration of wettability, by aging in crude oil at elevated temperature, produced chalk blocks which were strongly-water-wet and moderately-water-wet, but with identical pore geometry. Large scale, nuclear-tracer, 2D-imaging experiments monitored waterflooding through the blocks of chalk, first whole then fractured. Capillary pressure and relative permeabilities at each given wettability were experimentally measured and used as input for the simulations. Mixing of injection water and in-situ water was determined both for unfractured and fractured reservoirs by labeling the waters with different nuclear tracers.

For a low permeability increase after fracturing, for both unfractured and fractured chalk, the amount and rate of oil recovery by waterflooding were similar for strongly-water-wet and moderately-water-wet conditions, but the in-situ saturation distributions are shown to be significantly affected by wettability conditions. This indicates that the recovery mechanisms change towards more viscous dominant flow regimes at less water-wet conditions.

Introduction
To determine the impacts from wettability on oil recovery mechanisms in fractured reservoirs, scaled-up laboratory waterflood imaging experiments with corresponding numerical simulations have been performed. To investigate the simultaneous interaction between capillary forces, viscous forces and gravity and to reduce the impacts from capillary end effects, blocks of outcrop rock were used instead of core plugs. Imaging the local in-situ 2D-saturation development of the individual water compositions, the in-situ water and the injection water, the mixing of the waters was determined.

A previous series of laboratory waterflood experiments, using blocks of fractured chalk, where the advancing waterfront was tracked by the nuclear tracer 2D-imaging technique,[1-4] has shown that altering the wettability from strongly-water-wet to moderately-water-wet conditions had minor impacts on the amount and the rate of oil production. However, the in-situ saturation development was significantly different, indicating differences in oil recovery mechanisms.[5-7] The main objective for the current experiments was to determine the oil recovery mechanisms at different wettability conditions.

The term moderately-water-wet in this paper is defined to cover the wettability conditions reflecting an Amott-Harvey water index, I_w, in the range 0.5 – 0.8. Earlier we reported a technique that reproducibly altered wettability in outcrop chalk by aging the rock material in stock tank crude oil at elevated temperature for a selected period of time.[8] Utilizing this technique we have produced larger blocks of outcrop chalk at selected wettabilities, which were waterflooded, first as a whole block, then again after the blocks were fractured and reassembled. Earlier work reported on experiments using an embedded fracture network, while in this work two interconnected fracture networks, one that introduced hydraulic contact from inlet to outlet and one that also contained an isolated block surrounded by fractures, have been studied. Results on how injection water mixed with in-situ water improved the interpretation of the recovery mechanisms by providing information on the composition of the produced water.

A second objective of these experiments has been to validate a full field numerical simulator for prediction of the oil production and the in-situ saturation dynamics for these waterfloods. In this process quality control of the experimentally measured capillary pressure and relative permeability data, used as input for the simulator, has been performed at strongly-water-wet and moderately-water-wet conditions. Optimization of either P_c-data or k_r-curves for the chalk matrix in the numerical simulations of the whole blocks at different wettabilities gave indications of which of these input data could be most trusted. History matching both the production profile and the in-situ saturation distribution development gave higher confidence in the simulations than history matching the oil production only. In the numerical simulations of the waterfloods of the fractured blocks only the fracture representation was a variable.

Experimental

Rock and fluids

Five chalk blocks, CHP-4, CHP-8, CHP-9, CHP-12 and CHP-14, approximately 20 × 10 × 5 cm, were cut from large pieces of Rørdal outcrop chalk obtained from the Portland quarry near Ålborg, Denmark. Before the blocks were epoxy coated, local air permeability was measured at each intersection of a 1 × 1 cm grid on both sides of the blocks using a minipermeameter. The permeability maps indicated homogeneous blocks on a cm scale. The blocks were vacuum evacuated and saturated with brine containing 5wt% NaCl + 3.8wt% $CaCl_2$. Fluid data is found in Table 1. Porosity was determined from weight measurements and the permeability was measured across the epoxy coated blocks. Block data is listed in Table 2.

Initial water saturation

Initial water saturations, S_{wi}, of 22-28%PV were established for all blocks by oilflooding with a maximum differential pressure of 125 kPa/cm. In order to obtain a uniform, low S_{wi}, oil was injected alternately, at both ends. To add experience to the earlier work, emphasizing oil recovery in fractured chalk studying waterfloods of whole blocks and fractured blocks with embedded fracture networks,[5,6,8-18] the following experimental schedule was outlined: The waterfloods of the strongly-water-wet block CHP-4, with an embedded fracture network as shown in Figure 2b, was compared to a waterflood of the strongly-water-wet block CHP-9, with an interconnected fracture network as shown in Figure 2c. The strongly-water-wet block CHP-12, was waterflooded first as a whole block then again after it had been oilflooded back to S_{wi}, and then fractured and reassembled into the desired interconnected fracture network shown in Figure 2d. This experimental procedure was then repeated on the two blocks aged to moderately-water-wet conditions, CHP-8 and CHP-14. Block CHP-8 was waterflooded first as a whole block then with an embedded fracture network shown in Figure 2b and finally with an interconnected fracture network as shown in Figure 2c. CHP-14 was waterflooded as a whole block and then with the interconnected fracture network as shown in Figure 2d.

Oil flooding and aging

All blocks were oilflooded to approximately S_{wi} of 25%PV. The strongly-water-wet blocks were oilflooded using decane. Oilfloods of the moderately-water-wet blocks used stock tank crude oil from a chalk reservoir in the North Sea and were carried out at 90°C in a heated pressure vessel. The blocks were then aged under crude oil at 90°C for a designated time period. Because of possible wax problems with the crude oil used for aging, the temperature was maintained at 90°C as long as crude oil was in the block. After aging was completed, the crude oil was flushed out with decahydronaphthalene (decalin) which in turn was flushed out by n-decane at 90°C. Decalin was used as buffer between the decane and the crude oil to avoid asphaltene precipitation. Decane and brine were used during the waterfloods for all blocks.

Wettability testing

To get an initial indication of the wettability of the blocks aged in crude oil at 90°C to obtain moderately-water-wet conditions, duplicate core plug samples drilled from the same chunk of chalk that the block was taken from, received the same treatment as the blocks. A measure of the wettability was then obtained by the Amott-Harvey wettability test.[19] After the waterfloods of the blocks were terminated, core plugs were drilled out of each of the blocks and wettability measurements were conducted on the plugs. The aging process produced chalk blocks CHP-8 and CHP-14 at moderately-water-wet conditions, reflecting an Amott index to water, I_w, of 0.8 and 0.6, respectively. Thus we established five physical reservoir models with similar mineralogy and pore geometry but with different wettabilities.

Fractures

The fractures were created, when the whole block had been driven back to S_{wi} after the first waterflood, by cutting the block with a band saw. When reassembling the blocks, tape was placed over the fractures to prevent the epoxy, used to reseal the core, from entering the fractures. A 2 mm strip of Teflon was placed at the outer, lower, edge of the open fracture to assure a well defined open volume. A pressure of 10 kPa across the fractures was applied to mechanically hold the different parts of the block in position while the epoxy cured. The different fracture orientations and arrangements of the individual pieces for the reassembled blocks, are shown in Figure 2b-d. The xy coordinates are used to identify location. The individual blocks are identified as Block A1 and A2, the inlet blocks, Block B1 and B2, the central blocks which were surrounded by fractures and Block C1 and C2, the outlet blocks. Both an open fracture, no possible capillary contact, and several "closed" fractures, with contact between the adjacent matrix blocks, were formed. The "closed" fractures were intended to provide at least some capillary continuity of both fluid phases across the fracture. The open vertical fracture at 13 cm was created by sliding Block B1 and B2 to the left as far as possible producing an open fracture with the width of one saw cut, ca. 2 mm. The other fractures were "closed", i.e. the pieces were placed butt to butt when reassembling the block, with an axial force applied during the reassembly. After reassembly, the fracture network was filled with decane using a syringe. The interconnected fracture network assured hydraulic contact from the inlet to outlet end; i.e. from “injector” to “producer”. The blocks were positioned vertically during flooding, thus gravity was aligned with the vertical fractures.

Saturation monitoring

Nuclear-tracer, 2D-imaging experiments monitored waterflooding of the chalk blocks, first whole, then fractured. 2-D brine saturations were determined by measuring gamma ray emission from ^{22}Na and ^{60}Co separately dissolved in brines used alternately as injection water and in-situ water. Figure 1 shows the vertical 2D-flow rig used for saturation monitoring. The blocks were mounted in a vertical position while flooded and a saturation map was produced at each specified point in time, according to the grid shown in Figure 2. Each individual saturation map is identified by a scan number, cfr. e.g. Figure 3. Each scan number is preceded by a letter and number to identify each block, e.g. P12 and P14 for CHP-12 and CHP-14, respectively. The oil and waterfloods were labeled O and W, respectively, with the first digit being the flood number and the two digits following the dash indicating the chronological sequence of scans. Thus P12W2-09 is the 9th scan of the 2nd water flood on block CHP-12.

The working principle of the nuclear tracer technique has been described in detail elsewhere.[1-5] The outline of the experimental sequence used to flood the unfractured and fractured blocks, while using 2-D imaging to determine the distribution of brine saturation, and the results are summarized in Table 2.

The two tracers used for labeling the connate and injected water, are not ideal since both tracers are soluble in both fluids. However, the objective of this work was to look for development of a bank of the initial brine ahead of the connate brine. Mixing by diffusion and dispersion will be exaggerated due to the tracers being soluble in both of the brines. However, due to relatively short experiment duration it turned out that movement of the individual compositions could be readily identified.

Results and Discussion

Strongly-water-wet blocks

Waterfloods of whole blocks, both at strongly-water-wet and moderately-water-wet conditions have been shown to be similar with respect to oil production and in-situ saturation development.[5] Figure 3 and Figure 4 show how the water displaces the oil in a typical whole block waterflood. During all of the waterflood experiments the brine was injected from the left side of the image and the displaced fluids exited at the right side of the image. Figure 3 shows the dynamic saturation development for the injection water displacing the oil from the whole block CHP-12, Scans P12W1-00 to Scan P12W1-32. The corresponding dynamics for the in-situ water is shown in Figure 4. Uniform initial water saturation was measured for CHP-12 as the first saturation map, P12W1-00 in Figure 4. A dispersed waterfront flushed out 43%PV of decane. Increasing the flow rate has been shown to produce a less dispersed waterfront.[1] In waterfloods starting at higher initial water saturation there was essentially no waterfront at all, i.e. a uniform increase in water saturation was recorded.[13] A uniform final water saturation was obtained at ca. S_w=68%PV. As we have experienced earlier for core floods, the in-situ water banked up in front of the injection water, but compared to the earlier work, the banking was less pronounced and more dispersed, probably due to the lower flow rates applied in these block experiments. All of the in-situ water was displaced during the waterflood.

When the blocks were driven back to S_{wi} an excellent reproduction of the original water saturation and saturation distribution was generally obtained, see Table 2. Good agreement was obtained between the nuclear tracer determined in-situ saturation and mass balance.

The blocks were then cut with a band saw into the different configurations shown in Figure 2. The nuclear tracer saturation measurements of the whole and the assembled fractured block indicated that the cutting process did not measurably alter the saturation distribution at S_{wi}, as was also observed in previous experiments.[5,13,14]

Figure 5 shows the time development of the 2-D brine saturation during the constant differential pressure, 40 mbar, waterflood of the fractured block CHP-4. This was a Portland block cut with a hand saw, which gave a coarse surface to the fractures. The brine saturation increased as a dispersed front through Block A, the continuous inlet block, Scans P4W2-01 to P4W2-05. In Scan P4W2-05 Block B was still at, or close to, S_{wi} while the matrix just across the fracture in Block A was approaching S_{wf}. The brine did not appear to cross any of the fractures before the saturation in all of Block A was close to it's final water saturation. After Block A reached a high water saturation and the fractures were filled with brine, the brine entered Block B, Scan P4W2-06. The general appearance of the saturation distribution in Block B in Scan P4W2-06 suggested that the brine entered gradually from both the horizontal and vertical fractures between Block A and Block B. However, little, if any, water had crossed the 13 cm fracture into Block C at the time when Scan P4W2-07 was taken. When Block B approached it's final water saturation, water movement into Block C, the outlet block, was recorded, Scan P4W2-07. A higher water saturation in the lowest part of the Block C at the outlet-end, shown in scan P4W2-07, indicated possible gravity segregation in the open fracture. A prior experiment with Dania outcrop chalk, with the same fracture network, showed a significant effect of gravity in the open vertical fracture.[14] The reason for this difference can be attributed to a longer time between each individual scan. The vertical intensity bump at 13 cm, Scan P4W3-09, indicated that water collected at the bottom of the open fracture at 13 cm.

A previous constant flow rate water flood experiment on a block of Dania chalk[14] showed similar water flow pattern as obtained for the Portland block CHP-4. Even though the blocks were constructed from different types of chalk with significantly different matrix permeabilities, k=67 mD and k=2 mD for Dania and Portland, respectively, a consistent behavior was observed.

Figure 6 shows the experimental results of the time development of the total water saturation while waterflooding the fractured, strongly-water-wet block CHP-12. An interconnected fracture network that isolated blocks B1 and B2 was used (see Figure 2d). The brine saturation increased as a dispersed front through Block A2, the continuous inlet block, Scans P12W2-00 to P12W2-08. In Scan P12W2-08 Block B1 and B2 were still at, or close to, S_{wi} while the matrix just across the fracture in Block A1 and A2 was approaching S_{wf}. This suggested a limited rate of transport of fluids across the "closed" vertical fracture at 4 cm and the horizontal fracture at 5.0 cm. In fact the brine did not appear to cross any of the fractures before the saturations in all of Block A1 and A2 were close to their final water saturation. After Block A1 and A2 reached high brine saturations and the fractures were filled with brine, the brine entered Block B1 and B2, Scan P12W2-12. The general appearance of Block B1 and B2 in Scan P12W2-12 suggest that the brine entered gradually from both the horizontal and vertical fracture between Block A1 and A2 and Block B1 and B2. However, little, if any, water had gone across the fracture at 13 cm into Block C at the time when Scan P12W1-12 was taken. When Blocks B1 and B2 approached their final water saturation, water movement into Block C1 and C2, the outlet blocks, was recorded (see scan P12W2-17). Higher water saturation in the mid- to upper part of Block C2 at the outlet-end, shown in scan P12W2-17, indicated that the wetting phase crossed the “closed” fracture before any significant amount of water accumulated, by gravity segregation, in the bottom of the open fracture. The latter was observed in some earlier experiments performed at strongly-water-wet conditions.[5,13,14]

It has earlier been shown that there is essentially no difference in total oil recovery for a strongly-water-wet block between waterfloods on the whole block and a fractured block with embedded fractures.[5,13,14] In Figure 7 the oil production for the fractured block CHP-12, with interconnected fractures, is compared to earlier results on strongly-water-wet whole blocks and blocks with embedded fractures. From the figure it is evident that water breakthrough in the block with interconnected fractures occurred somewhat earlier and the block produced slightly less oil. The hydraulic contact from inlet to outlet also resulted in a short period with two-phase production, giving less sharp water cut. This trend is more noticeable for the higher permeability increase with connected fractures, but the reduction in oil recovery is still minor. A total of 42%PV oil was produced. We interpret this as a result of the recovery mechanisms being controlled by spontaneous imbibition and thus the endpoint saturation is predominantly determined by the capillary forces.

Moderately-water-wet blocks

Block CHP-8 was treated to provide moderately-water-wet conditions, although it turned out to be more water-wet than expected. Results on waterflooding CHP-8 can be found in Ref. 6. The main conclusion from waterflooding this block first as a whole block, second with embedded fractures and third, with interconnected fractures, was that even at a wettability of I_w=0.8 the in-situ saturation development for the waterfloods of the fractured block showed the same behavior previously seen for the less-water-wet conditions.[5,6] This implied that the wetting phase crossed the fractures early and no significant capillary hold-up at the fracture, as observed at strongly-water-wet conditions, were recorded.[5,6,14]

The moderately-water-wet block CHP-14 (I_w=0.6) was waterflooded first as a whole block, and then with an interconnected fracture network. For the whole block waterflood, a dispersed water front swept out 43%PV of oil from the block. As for the waterflood of the strongly-water-wet whole block CHP-12, significant banking of the in-situ water was observed and all of the in-situ water was displaced for the whole block waterflood of CHP-14.

Figure 8 shows the time development of the injected brine saturation during the waterflood of the moderately-water-wet fractured block, CHP-14, with the interconnected fracture network shown in Figure 2d. The brine saturation increased as a dispersed front through Block A1, the upper continuous inlet block, and into Block B1 and B2, (Scans P14W2-00 to P14W2-10). In contrast to earlier experiments of waterflooding moderately-water-wet fractured blocks, the fractures had significant effect; transport of fluids along the fractures was observed and water accumulated in the bottom of the open fracture at 13 cm. This was probably due to a higher permeability increase after fracturing, compared with earlier experiments at moderately-water-wet conditions. The permeability to water at Sor increased by a factor of 11 relative to the whole block. However, some capillary contact across the "closed" fractures had apparently been established, as had been the case in earlier experiments. Gravity segregation in the open vertical fracture was observed. The water entered Block C2 from the bottom of the open fracture and across the "closed" vertical fracture at 13 cm.

The dynamic behavior of the in-situ water while waterflooding fractured block CHP-14 is shown in Figure 9. The in-situ water was gradually displaced, but no banking was recorded. Even after 1.0 PV of water had been injected, more than 10%PV of in-situ water remained, particularly in the isolated blocks B1 and B2. This indicated that after fracturing, less injection water was flushed through the matrices, thus causing the displacement of in-situ water to be less efficient.

Oil production from waterfloods on the whole and fractured moderately-water-wet block CHP-14 is shown in Figure 7. For the whole block, at moderately-water-wet conditions, oil recovery was similar to the whole blocks at strongly-water-wet condition. When fractured, the block showed earlier water breakthrough and a longer transition zone with two-phase production. Less oil, 32%PV, was produced.

This behavior, that total oil recovery from each block was reduced by a consistent, but small amount, after fracturing the blocks as long as the permeability increase was low, is consistent with results for all the different wettability conditions reported in Ref. 5. At strongly-water-wet conditions, a permeability increase after fracturing of about 50 did not reduce the oil production compared to the baseline whole block experiment, as recorded for block CHP-9. Even a permeability increase of about 200, as for block CHP-12, did not reduce the oil production by any significant amount, for the fractured strongly-water-wet blocks. At moderately water-wet conditions, however, the reduction in oil production was about 10%PV, when the effective water permeability at Sor increased after fracturing by a factor of about 10.

The pattern of water movement during the first waterflood of the strongly-water-wet, fractured block CHP-12, indicated that there was little capillary contact, for the water phase, between Blocks A2 and C1 and C2 across the upper portion of the fracture at 13 cm. If there had been significant capillary continuity, water would have readily crossed the fracture and saturated the upper portion of Block C1 and C2 during the early stages of invasion of Block A. However, gravity segregation of the fluids in the fractures indicated fairly open fractures at 13 cm for CHP-12. For the less water-wet blocks, CHP-14 and CHP-8, the water entered Block C1 and C2 both from the bottom of the open fracture and from the "closed" vertical fracture at 13 cm. This indicated a combined effect resulting from the fracture enhanced permeability and reduced influence of the "closed" fractures on the flow pattern during waterflood when the wettability changed towards moderately-water-wet. It seems unlikely that this was due to better capillary contacts between the blocks in CHP-14 and CHP-8, since the reassembling procedure was similar for all the blocks, and this effect has been consistently observed in earlier experiments. We speculate that a) capillary holdup of the wetting phase at less water wet conditions is reduced or b) that water droplets are being formed at the exit end of the block and establish wetting phase bridges across the fractures when the contact angle increases as wettability is changed to less water-wet conditions. The latter displacement mechanism depends on the fracture aperture, the viscous pressure in the wetting phase, i.e. the applied differential pressure and the wettability conditions. We believe one of these two mechanisms or a combination of the two are responsible for the reduced impact of the fractures on the water floods at less-water-wet conditions.

Numerical Simulations

Capillary pressure and relative permeability have been measured in chalk core plugs at strongly-water-wet, moderately-water-wet and nearly-neutral-wet conditions.[18] Plug wettability was selectively altered by aging outcrop chalk plugs, at S_{wi}, in crude oil at an elevated temperature for selected periods of time. This procedure reproduced the desired wettability while keeping the pore network structure and the mineralogy constant. Aging to a less-water-wet state significantly reduced spontaneous brine imbibition rate and endpoint. However, it did not reduce the total movable oil, i.e. imbibition plus forced displacement. In fact, the total movable oil generally increased slightly with reduced water wettability, however, at the cost of higher differential pressures. Reduced water wettability also lowered the drainage threshold pressure. Reproducibility of repeat imbibition tests on individual plugs indicated that the wettability alteration was permanent. These experiments were conducted in order to obtain input data for capillary pressure and relative permeability at a range of wettability conditions for numerical simulations. A full field simulator for fractured reservoirs, SENSOR (Ref. 20), was used to simulate numerically oil recovery from the fractured blocks. First, the simulations were run using experimental values for both capillary pressure and relative permeabilities at the different wettabilities. Then, to improve the history matching for both the oil production and the dynamics of the in-situ saturation development, the input data was adjusted. Capillary pressure curves were optimized while keeping the experimentally derived relative permeabilities constant and then the relative permeabilities were optimized with the experimental capillary pressure curves held constant. This procedure gave an indication of the validity of the measured values. The overall best match with the experiments for all the simulations was always obtained using the experimentally obtained capillary pressure curves and optimized relative permeabilities.

Figure 10 shows the resulting history match for the local water saturation development in the block during waterflooding the whole block CHP-12. Figure 11 shows the match of the oil production when waterflooding the whole block CHP-12 and when it was fractured. In the right side of Figure 12 the simulation of the local saturation development during the waterflood of the fractured block CHP-12 is compared to the experimental result of this waterflood. A satisfactory history match was obtained.

Conclusions

From two-dimensional in-situ saturation development during waterfloods at strongly-water-wet and at moderately-water-wet conditions in large fractured blocks of chalk the following conclusions can be drawn:

- Water movement during water flooding was significantly affected by the presence of fractures at strongly water-wet conditions, but not at moderately-water-wet conditions.
- For unfractured and fractured chalk the oil recovery by waterflooding was similar for strongly-water-wet chalk and moderately-water-wet chalk, when the permeability increase after fracturing was low.
- Production rate and total oil production was not affected by fractures at strongly-water-wet conditions, but for moderately-water-wet chalk oil recovery was reduced when the permeability increase after fracturing was high.
- Open fractures act as barriers to flow at strongly-water-wet and moderately-water-wet conditions.
- Experimentally obtained P_c and k_r input data have been evaluated by history matching in-situ saturation distribution development as well as the production profile. The overall best match between the simulations and the experiments was obtained using the experimentally obtained capillary pressure curves and optimizing the relative permeabilities.
- A simulator for fractured reservoirs was validated by large scale experiments with 2D-in-situ imaging information.
- The recovery mechanisms changed towards more viscous dominant flow regimes at less-water-wet conditions; this was even observed in fractured blocks.

Nomenclature

D= diameter [cm]
I= Amott wettability index
k= permeability [md]
L= length [cm]
p= paper
P= Pressure [bar]
R= oil recovery [%]
S= saturation
t= time [days]
T= temperature [°C]

Greek
m= viscosity [cp]
r= density [g/cm3]
s= interfacial tension, [IFT]
j= porosity[%]

Subscripts
a= aged
C= capillary
d= displacement
eff= effective
f= final
i= initial
im= imbibition
o= oil
si= spontaneous imbibition
w= Amott wettability index
k= permeability [mD]
S= saturation
w=water

References

1. Lien, J.R., Graue, A. and Kolltveit, K.: "A Nuclear Imaging Technique for Studying Multiphase Flow in a Porous Medium at Oil Reservoir Conditions", Nucl. Instr. & Meth., A271, 1988.
2. Graue, A., Kolltveit, K., Lien, J.R. and Skauge, A.: "Imaging Fluid Saturation Development in Long Coreflood Displacements", *SPEFE*, Vol. 5, No. 4, 406-412, (Dec., 1990).
3. Graue, A.: "Imaging the Effect of Capillary Heterogeneites on Local Saturation Development in Long-Core Floods", *SPEDC*, Vol. 9, No. 1, March 1994.
4. Bailey, N.A., Rowland, P.R., Robinson, D.P.: "Nuclear Measurements of Fluid Saturation in EOR Flood Experiments", Proc.: 1981 European Symposium on Enhanced Oil Recovery, Bornmouth, England, Sept. 21-23, 1981.
5. Graue, A., Viksund, B.G., Baldwin, B.A., Spinler, E.: "Large Scale Imaging of Impacts of Wettability on Oil Recovery in Fractured Chalk", *SPE Journal*, Vol. 4, No. 1, March 1999.
6. Graue, A., Bognø, T.: "Wettability Effects on Oil Recovery Mechanisms in Fractured Reservoirs", SPE56672, 1999 SPE Annual Tech. Conf. And Exh., Houston, TX, Oct. 3-6, 1999.
7. Graue, A., Moe, R.W., Baldwin, B.A.: "Comparison of Numerical Simulatons and Laboratory Waterfloods with In-Situ Saturation Imaging of Fractured Blocks of Reservoir Rocks at Different Wettabilities", SPE59039, 2000 SPE Internatl. Petr. Conf. And Exh., Villahermosa, Mexico, Febr. 1-3, 2000.
8. Graue, A., Viksund, B.G., Baldwin, B.A: "Reproducible Wettability Alteration of Low-Permeable Outcrop Chalk", *SPE Res. Eng. and Eval*., April, 1999.
9. Graue, A. and Viksund, B.G.: "Imaging Immiscible Two Phase Flow in Low Permeability Chalk – Emphasis on Recovery Mechanisms and Scaling", Ext.Abs.Proc.: EAPG/AAPG Special Conference on Chalk, Copenhagen, Denmark, (Sept. 7-9, 1994).
10. Graue, A.: "Nuclear Tracer Saturation Imaging of Fluid Displacement in Low-Permeability Chalk", SPE 25899, Proc.: SPE Rocky Mountain Regional/Low Permeability Reservoirs Symposium, Denver, CO, USA, (April 26-28, 1993).
11. Viksund, B.G., Hetland, S., Graue, A. and Baldwin, B.A.: "Imaging Saturation during Flow in Fractured Chalk: Emphasizing Recovery Mechanisms, Capillary Continuity and Scaling", Reviewed Proc.: 1996 Int. Symp. of the Society of Core Analysts, Montpellier, France, (Sept. 8-10, 1996).
12. Torsaeter, O.: "An Experimental Study of Water Imbibition in Chalk from the Ekofisk Field", SPE 12688, Proc.: SPE/DOE Fourth Symposium on EOR, Tulsa, OK, (April 1984).
13. Viksund, B.G., Graue, A., Baldwin, B. And Spinler, E.: "2-D Imaging of waterflooding a Fractured Block of Outcrop Chalk". Proc.: 5th Chalk Research Symposium, Reims, France, (Oct. 7-9, 1996).
14. Viksund, B.G., Eilertsen T., Graue, A., Baldwin, B. and Spinler, E.: "2D-Imaging of the Effects from Fractures on Oil Recovery in Larger Blocks of Chalk", Reviewed Proc.: International Symposium of the Society of Core Analysts, Calgary, Canada. (Sept. 8-10, 1997).
15. Graue, A., Tonheim, E. and Baldwin, B.: "Control and Alteration of Wettability in Low-Permeability Chalk", Proc.: 3rd International Symposium on Evaluation of Reservoir Wettability and Its Effect on Oil Recovery, Laramie, Wy., USA, Sept., 1995.

16. Viksund, B.G., Morrow, N.R., Ma, G., Wang, W., Graue, A.: «Initial Water Saturation and Oil Recovery from Chalk and Sandstone by Spontaneous Imbibition», reviewed proc.: 1998 International Symposium of Core Analysts, The Hague, Sept., 1998.
17. Spinler, E.A, Baldwin B. A., Graue, A.: "Simultaneous Measurement of Multiple Capillary Pressure Curves from Wettability and Rock Property Variations Within Single Rock Plugs", SCA9957, Reviewed Proc.: 1999 International Symposium of Core Analysts, Golden, Co., USA, Aug. 1-4, 1999.
18. Graue, A., Bognø, T., Moe, R.W., Baldwin, B.A., Spinler, E.A., Maloney, D., Tobola, D.P.: "Impacts of Wettability on Capillary Pressure and Relative Permeability", SCA9907, Reviewed Proc.: 1999 International Symposium of Core Analysts, Golden, Co., USA, Aug. 1-4, 1999.
19. Amott. E.: "Observations Relating to the Wettability of Porous Rock", *Trans*., AIME 1959 216, 156-162.
20. Coats, K.H., Thomas, L.K., and Pierson, R.G.: "Compositional and Black Oil Reservoir Simulation", SPE29111, 13th SPE Reservoir Simulation Symposium, San Antonio, Texas, Febr. 1995.

Table 1. Fluid properties.

Fluid	Density [g/cm^3]	Viscosity [cP] at 20°C	Viscosity [cP] at 90°C	Composition
Brine	1.05	1.09		5 wt% NaCl + 3.8 wt% $CaCl_2$
n-Decane	0.73	0.92		
Decahydronaphtalene	0.896			
Crude oil	0.849	14.3	2.7	

Table 2. Experimental data for chalk blocks.

Block	CHP-4		CHP-8			CHP-9		CHP-12		CHP-14	
Outcrop	Portland		Portland			Portland		Portland		Portland	
Location	Ålborg		Ålborg			Ålborg		Ålborg		Ålborg	
Length (cm)	20		19,9			19,8		20,0		20	
Height (cm)	13		10,0			10,0		10,0		10,0	
Thickness (cm)	5,5		5,5			5,4		5,0		5	
Abs. Permeability (mD)	1,8		2,3			3,8		2,3		2,2	
Porosity (%)	45,0		47,6			48,1		45,7		46,2	
Pore Volume (ml)	648		516			514		457		450	
MISC. FLOOD # :	1		1			1		1		1	
Flow Rate (ml/hr)	25		10			40		15		20	
OILFLOOD # :	1	2	1	2	3	1		1	2	1	2
Oil Viscosity (cP)	0,92	0,92	2,7	0,92	0,92	0,92		0,92	0,92	2,7	0,92
Swi (%PV)	100	65	100	76	72	100		100	67	100	71
dSw (%PV)	73	39	72	43	37	73		76	44	72	49
Swf (%PV)	27	26	28	33	35	27		24	23	28	22
Max Pressure (Bar)			10	24	24	24		25	25	9,5	25
Endpoint Eff. Perm. to oil (mD)	1,7	1,6^a/4,6^b	3	1,3^a/1,3^b	1,0^b/42^c	3,3^a/156^b		2,5	2,4^a	0,4	2,4^a
AGING :	No		YES			NO		NO		YES	
Aging Temp. (deg. C)			90							90	
Aging Time (days)			83							1,6	
Amott index after aging	1,0		0,53			1,0		1,0		0,6	
Oil flooding prior to imb. :											
Decaline (PV)			5							5	
n-Decane (PV)			5							5	
Endpoint eff. Perm. to oil (mD)			2,4							0,4	
WATERFLOOD # :	1	2	1	2	3	1	2	1	2	1	2
Block Condition	Whole	Fractured	Whole	Fractured	Fractured	Fractured	Fractured	Whole	Fractured	Whole	Fractured
Cutting		Hand Saw		Band Saw	Band Saw	Band Saw	Band Saw		Band Saw		Band Saw
Oil Viscosity (cP)	0,92	0,92	0,92	0,92	0,92	0,92	0,92	0,92	0,92	0,92	0,92
Swi (%PV)	27	26	28	33	35	27	67	24	23	28	22
dSw (%PV)	38	40	45	39	40	40	1	44	42	43	32
Swf (%PV)	65	66	73	72	75	67	68	67	65	71	54
Endpoint Eff. Perm. to water (mD)	0,4	0,6	0,4	0	15	87^b	42	0,7	155	0,2	2,2
Oil Recovery (%OIP)	52	54	63	58	62	55	3	57	55	59	41
Flow Rate / Const. Pres. (ml/hr / mbar)	- / 40	- / 40	1 / -	1 / -	1 / -	1 / -	20 / -	1 / -	1 / -	1 / -	1 / -

a) Whole block
b) Fractured block, embedded fracture network
c) Fractured block, interconnected fracture network

Figure 1. The vertical flowrig at the University of Bergen.

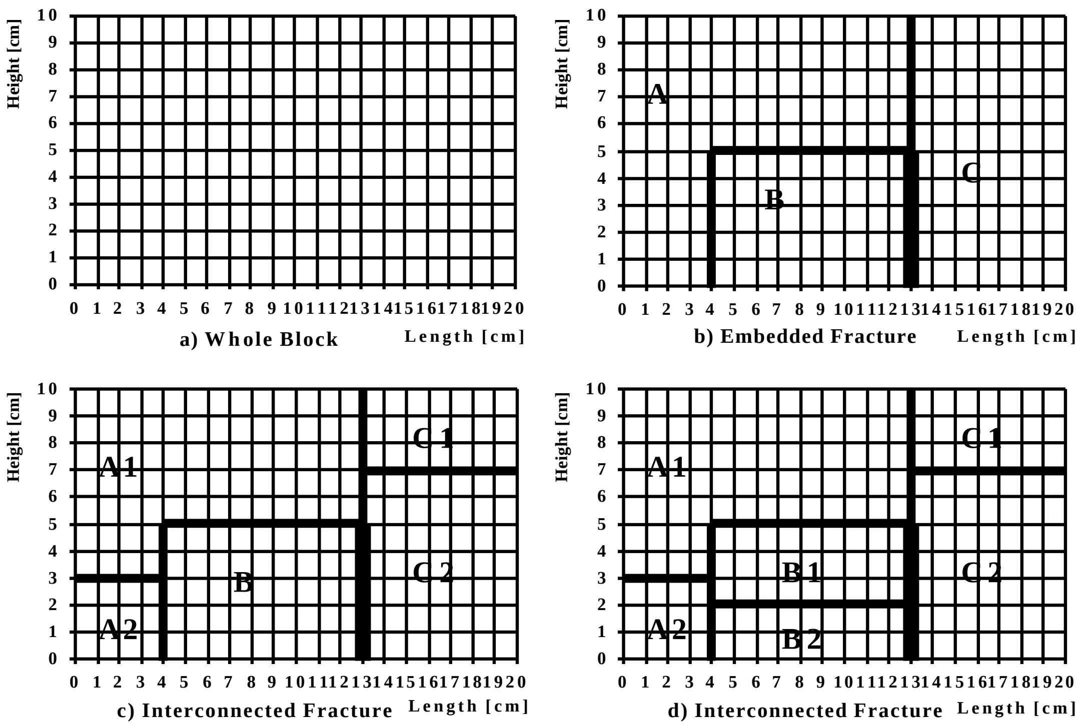

Figure 2. The fracture networks used in the experiments and the simulations.

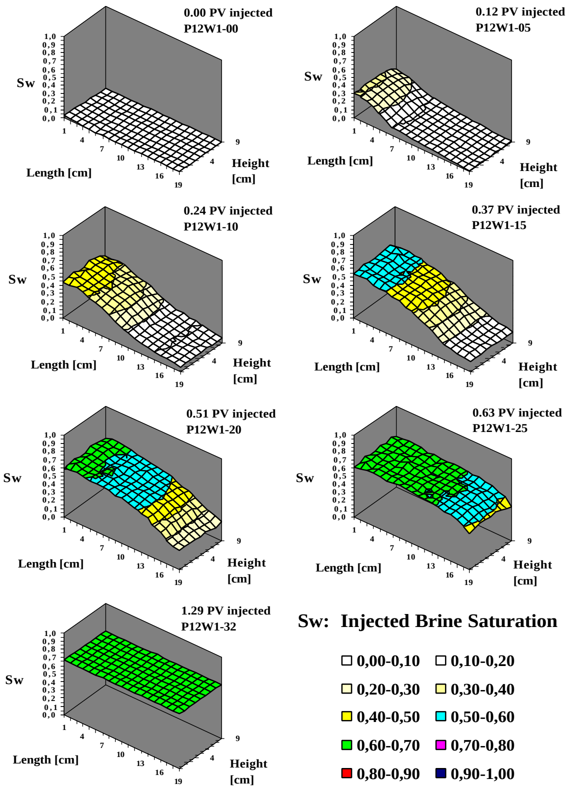

Figure 3. Saturation development of the injected water while waterflooding whole block CHP-12.

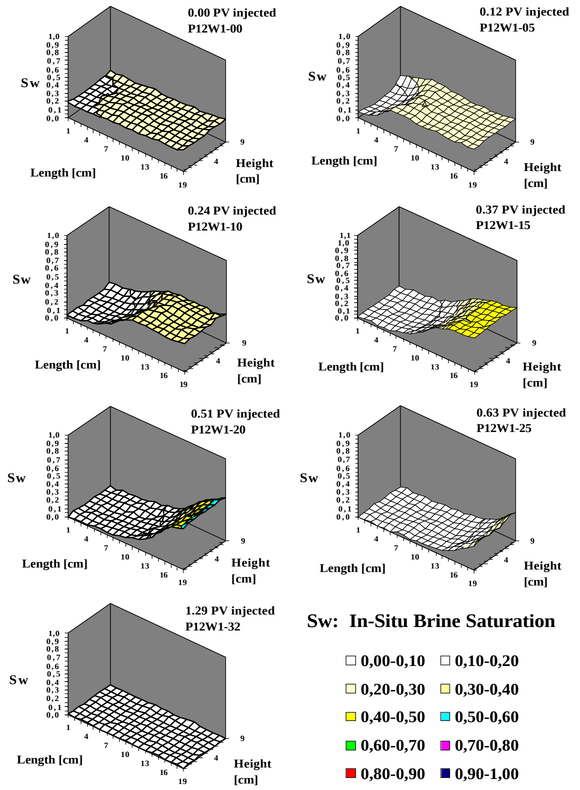

Figure 4. Saturation development of the in-situ water while waterflooding whole block CHP-12.

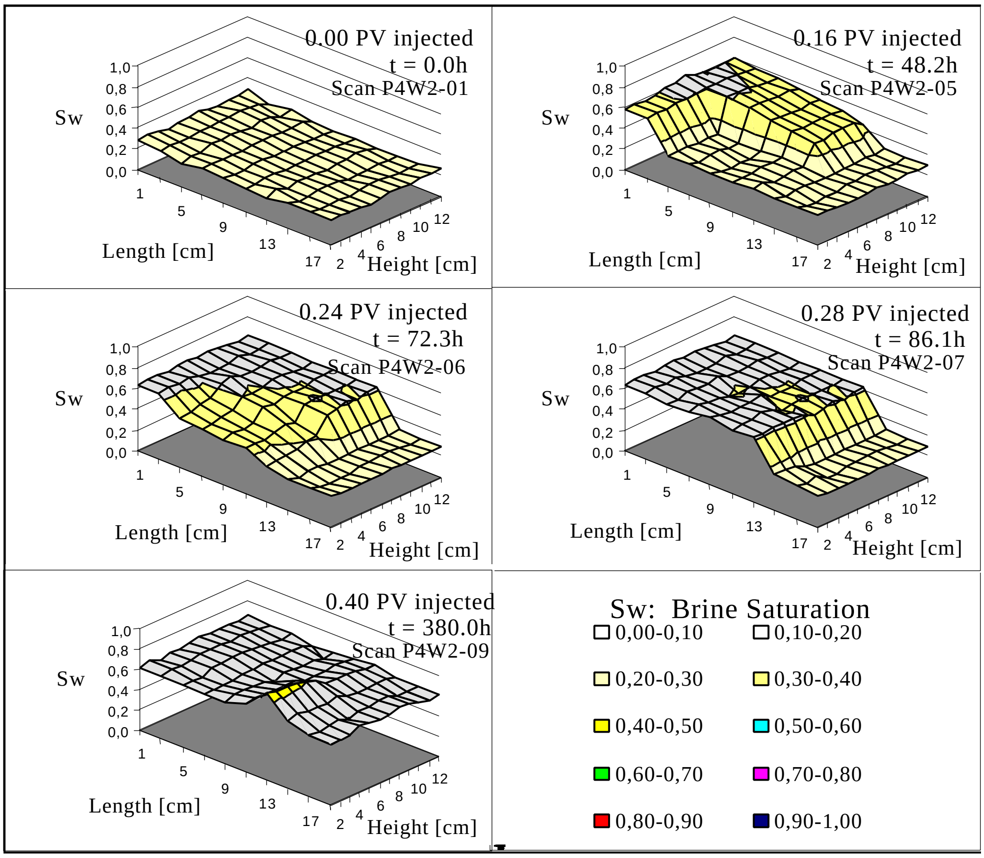

Figure 5. Water saturation development while waterflooding the fractured block CHP-4.

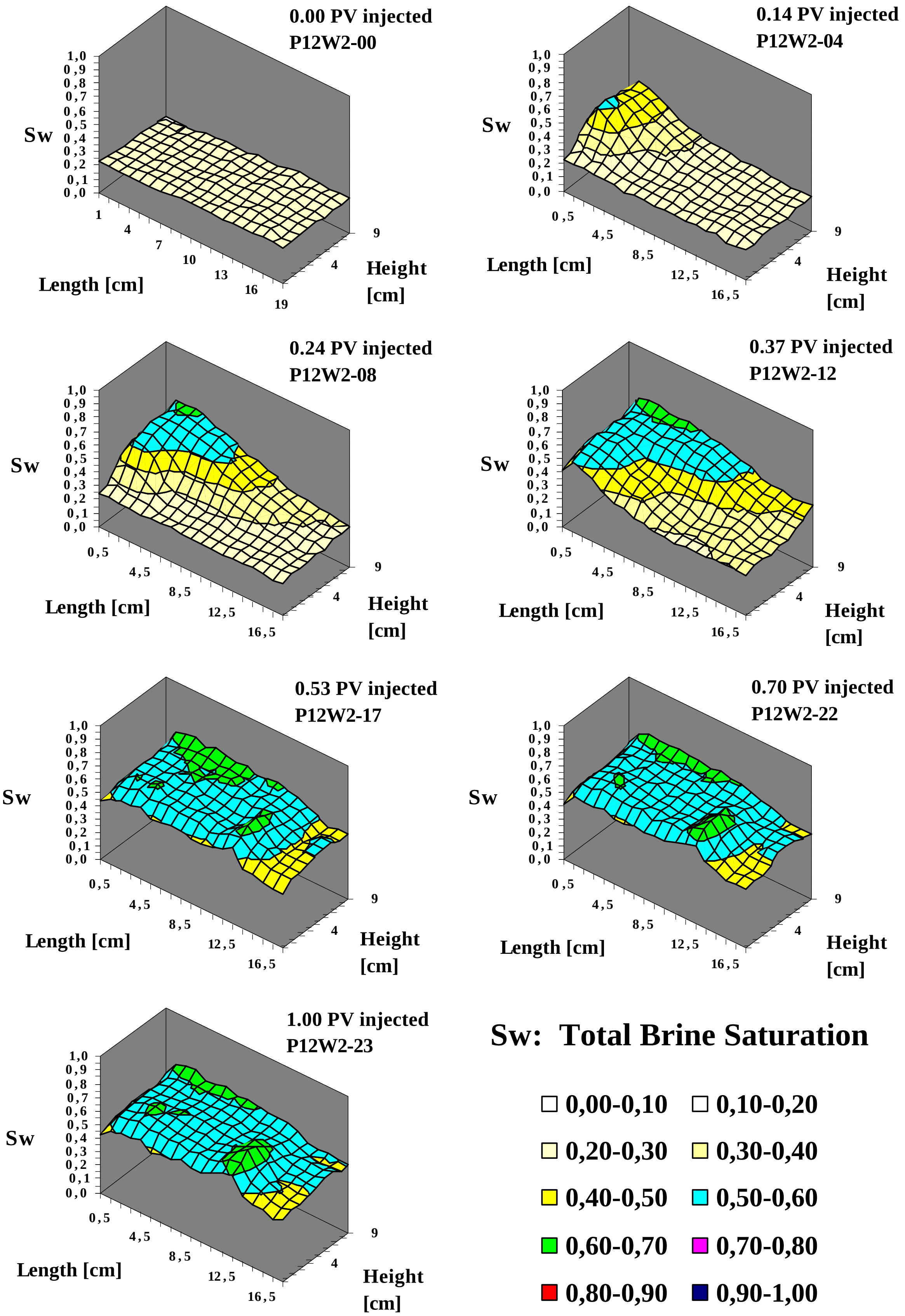

Figure 6. Saturation development of the total water while waterflooding fractured block CHP-12.

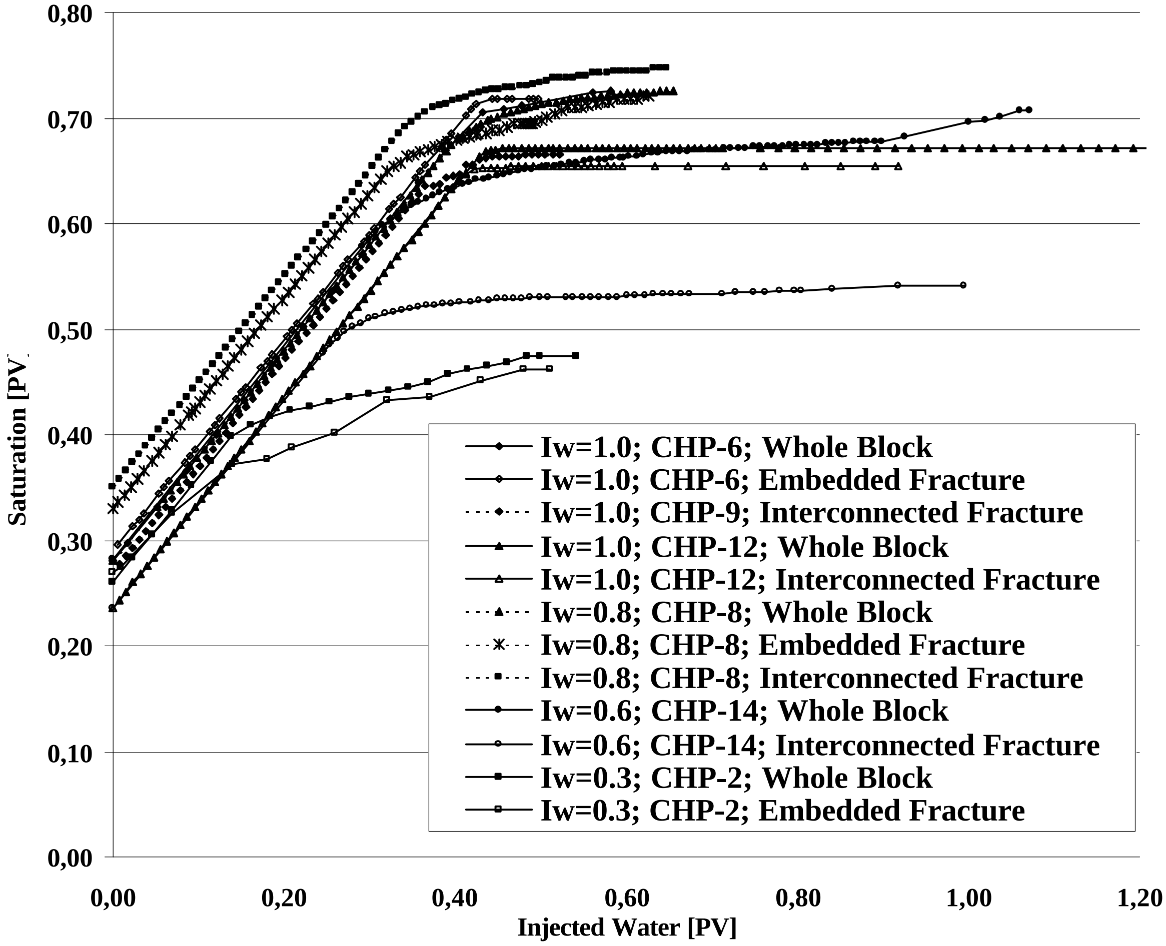

Figure 7. Water saturation when waterflooding whole and fractured block CHP-2 (Ref. 5), CHP-6 (Ref. 5), CHP-8, CHP-9, CHP-12 and CHP-14.

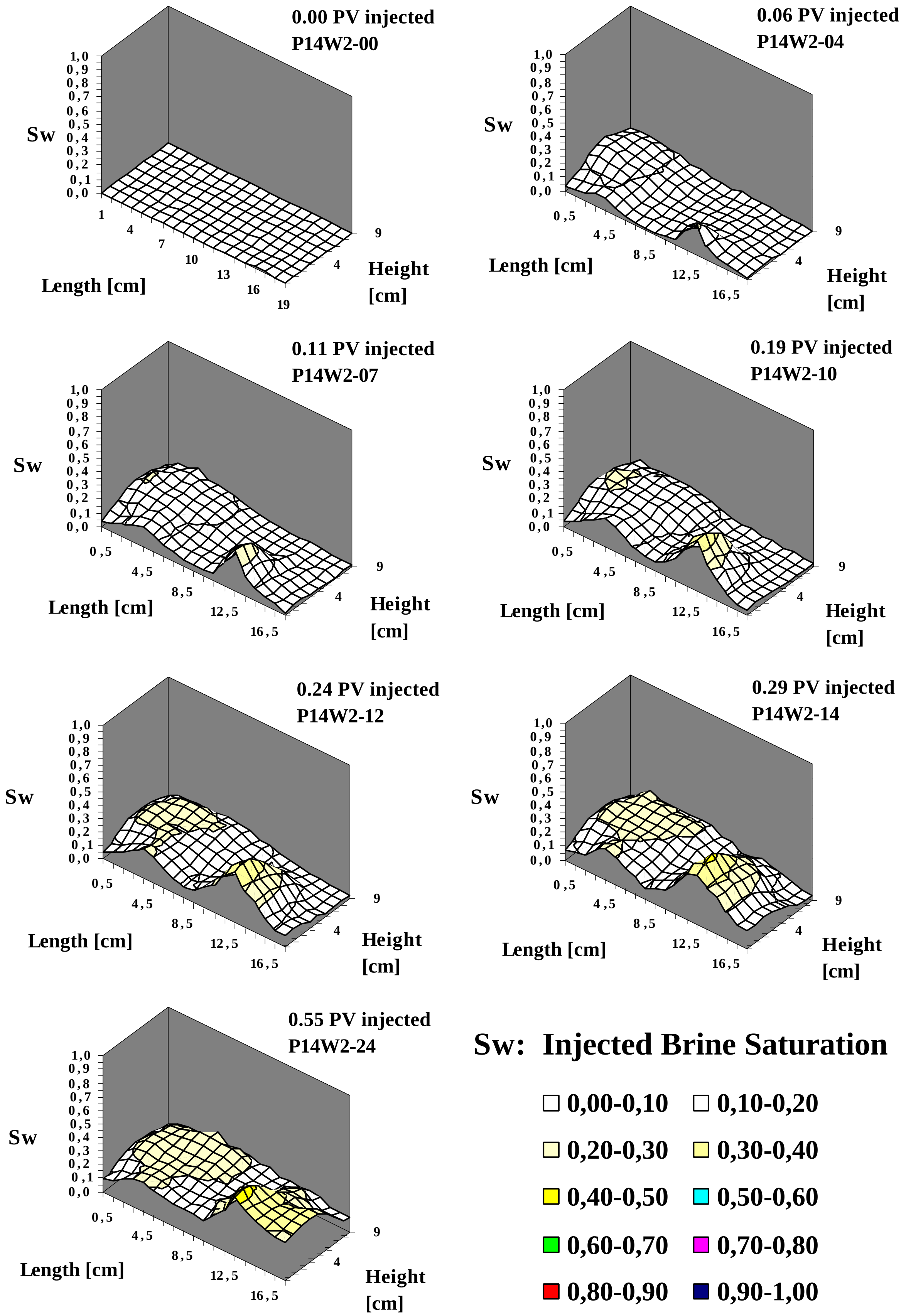

Figure 8. Saturation development of the injected water while waterflooding fractured block CHP-14.

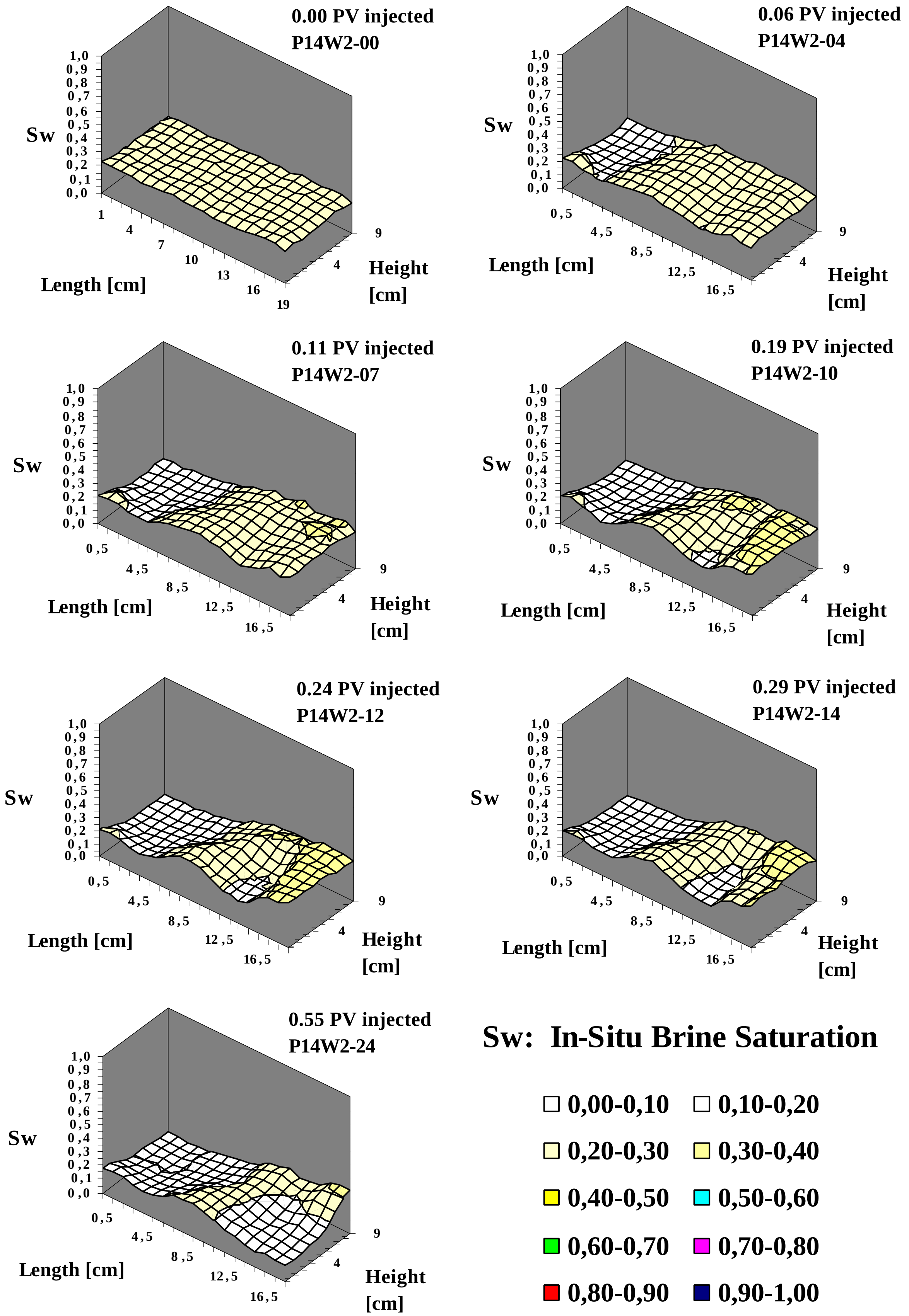

Figure 9. Saturation development of the in-situ waterwhile waterflooding fractured block CHP-14.

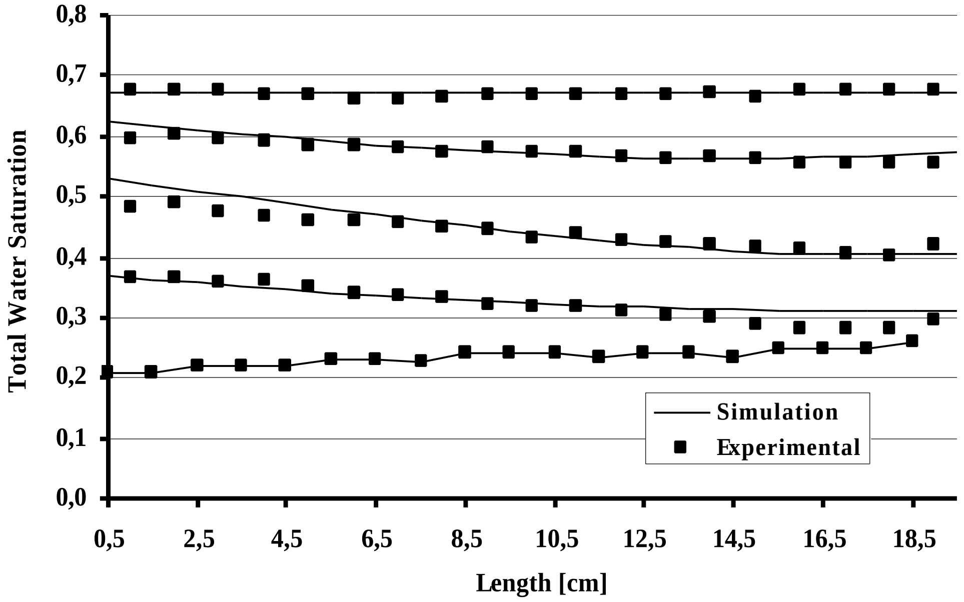

Figure 10. Comparison of experimental and simulated water profiles averaged over cross section of block, when waterflooding whole block CHP-12.

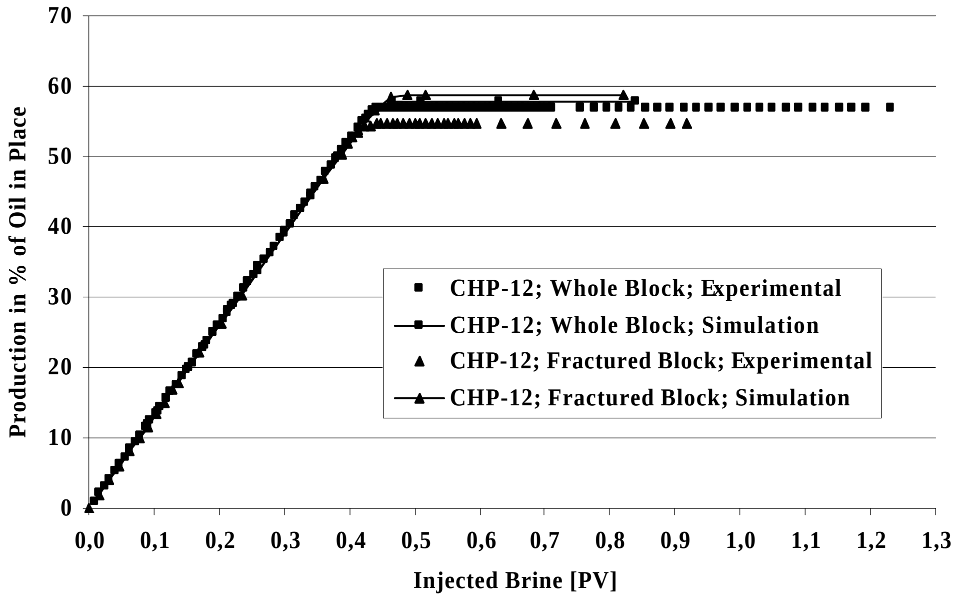

Figure 11. Experimental and simulated oil production when waterflooding both whole and fractured block CHP-12.

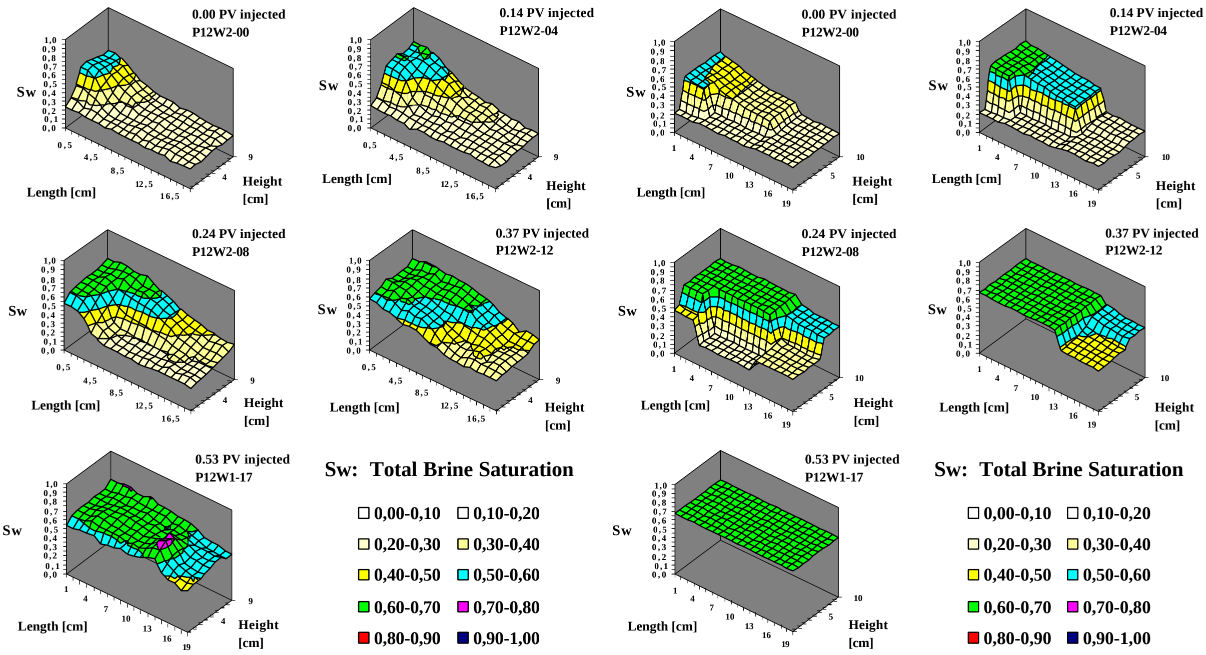

Figure 12. Comparison of experimental, left two columns, and simulated, rightmost two columns, in-situ saturation development for the second waterflood of the strongly water-wet block CHP-12.